LMI-Based Stubborn and Dead-Zone Redesign in Linear Dynamic Output Feedback

Sophie Tarbouriech, *Senior Member, IEEE*, Angelo Alessandri, *Senior Member, IEEE*,
Daniele Astolfi, and Luca Zaccarian, *Fellow, IEEE*

Abstract—**The redesign of output feedback controllers for linear systems based on adaptive saturation (stubborn) and dead-zone redesign is investigated by showing that input-to-state stability holds in closed loop upon the satisfaction of linear matrix inequalities. Such results are obtained by using sector conditions that are involved in the Lyapunov analysis in order to ensure input-to-state stability. A simulation case study shows the effectiveness of the proposed redesign in denoising and outlier attenuation with increased accuracy and precision.**

Index Terms—**Saturation, dead-zone, sector conditions, LMI.**

I. INTRODUCTION

DISTURBANCE attenuation in feedback design is of primary importance in control applications. For linear systems, many techniques have been developed in output feedback control, such as $\mathcal{H}_\infty$, $\mathcal{H}_2$ design or LQG approaches [1]–[3]; geometric approaches [4]; or internal-model based regulators [5]. Often a state-feedback design is combined with a state observer, but purely output feedback regulators can be also obtained [6]. Linear controllers posses however structural performance limitations [3, Chs. 5 and 6]. A possible way to overcome such limitations is to use nonlinear or hybrid techniques. We recall the works [7]–[11] as few examples of hybrid controllers employed for performance improvement by means of reset or switching strategies. Here we pursue instead the use of a nonlinear device for output feedback control of linear systems, while providing solid theoretical findings in terms of input-to-state stability (ISS, [12]) properties.

In this letter, we propose two redesign methods for dynamic output feedback of linear systems by embedding *stubborn*

(saturation) and *dead-zone* redesign techniques [13]–[18] in an output feedback loop to improve noise reduction. Our goal is twofold: with a stubborn redesign, we improve the transient response of the closed loop to measurement outliers. Instead, with a dead-zone redesign, we get a reduction in the sensitivity of the closed loop to persistent disturbances such as measurement bias or Gaussian noise affecting the output. Our solution extends the above-mentioned observer design techniques by adopting an output feedback term (rather than the output injection term) with a saturation or a dead-zone function having a variable threshold, adapted according to a linear filter dynamics. The series of works [13]–[16] have highlighted the potential of this paradigm in the context of observers. We show here that, by redesigning a given output feedback controller, not only the original ISS properties are preserved, but also the overall performances can be improved.

It has been already shown in the case of asymptotic observers (output injection), the stubborn redesign is particularly efficient in the presence of outliers affecting the measured outputs [13]–[15], while the dead-zone redesign helps in robustifying the observer against high-frequency measurement noises [15], [16]. In fact, [13] and [16] initially motivated the construction of these nonlinear redesigns in the context of linear observers. Later, the stubborn paradigm was extended to synchronization of multi-agent systems [17], [18], set-membership estimation [19], low-power high-gain observers [20], extended Kalman filtering [21], estimation for distributed parameter systems [22], nonlinear filtering [23]. Here instead, we extend the approach to a generic linear output feedback (possibly dynamic) controller, exploiting linear matrix inequalities (LMIs) [24] for the parameter tuning, generalizing the output injection scenarios of [13] and [16]. In particular, we allow in our setting for any given stabilizing linear dynamic output feedback law designed for a multivariable linear plant affected by disturbances, and provide LMI-based stubborn/dead-zone redesign conditions that guarantee closed-loop exponential ISS. The feasibility of our LMI-based conditions is also proven. Performance improvements are shown via a simulation example inspired from a model of the longitudinal dynamics of a fixed-wing vehicle flying at high speed [25].

The rest of this letter is structured as follows. In Section II we state the problem formulation. In Section III the stubborn redesign is addressed, while the Section IV studies the dead-zone redesign. Conclusions are drawn in Section V.

Notation: $\mathbb{R}_{\geq 0}$ denotes the set of non-negative real numbers. For a vector x or a matrix A, $x^\top$ and $A^\top$ denote their transposes, respectively. $x_{(i)}$ and $A_{(i)}$ denote the ith component of vector x and the ith row of matrix A, while $|x| := \sqrt{x^\top x}$ denotes the Euclidean norm of x and diag(x) is a diagonal matrix having diagonal elements $x_{(i)}$. For two symmetric matrices A, B of equal dimensions, $A > B$ means that $A - B$ is (symmetric) positive definite. For a square matrix A, He$(A) = A + A^\top$, $\lambda_{\max}(A)$ (resp. $\lambda_{\min}(A)$) denotes the maximal (resp. minimal) eigenvalue of matrix A. I and 0 stand for the identity and the null matrix of appropriate dimensions, respectively. For a partitioned matrix, the symbol $\star$ stands for symmetric blocks. Given two vectors x_1, x_2, we denote $(x_1, x_2) = [x_1^\top \ x_2^\top]^\top$.

II. PROBLEM FORMULATION

Consider the following linear plant

$$\dot{x}_p = A_p x_p + B_p u + B_{pw} w$$
$$y = C_p x_p + D_{pw} w, \tag{1}$$

where $x_p \in \mathbb{R}^{n_p}$ is the state, $u \in \mathbb{R}^m$ is the control input, $w \in \mathbb{R}^{n_d}$ is an exogenous disturbance input (comprising process disturbances and measurement noise), and $y \in \mathbb{R}^p$ is the measured output. Matrices A_p, B_p, B_{pw}, C_p, and D_{pw} are constant known matrices of appropriate dimensions.

We assume that for plant (1) a linear stabilizing dynamic output feedback controller has been designed, as follows

$$\dot{z} = Fz + Gy$$
$$u = Hz + Ny, \tag{2}$$

where $z \in \mathbb{R}^{n_c}$ is the state of the dynamic controller and F, G, H, and N are constant matrices of appropriate dimensions. For closed loop (1)-(2) we enforce the following mild assumption, which is not restrictive.

Assumption 1: The linear closed-loop system (1)-(2) with $w \equiv 0$ is globally exponentially stable to the origin.

Assumption 1 only holds if the triplet (A_p, B_p, C_p) be stabilizable and detectable: a necessary assumption for output feedback stabilizability (with a linear feedback). The assumption is also sufficient and necessary to guarantee global exponential stability with our mildly invasive redesign solutions.

Inspired by the recent works [13]–[16] where linear and nonlinear observers are augmented with dynamic saturations or dead-zones acting on the output injection term, we follow a similar paradigm for the case of output feedback augmentation.

III. LMI-BASED STUBBORN REDESIGN

A. Design Paradigm and Main Result

With measurement outliers, namely sporadic large-amplitude disturbances affecting the measurement output y, we redesign the closed loop (1)-(2) by augmenting controller (2) with a new non-negative state $\sigma \in \mathbb{R}_{\geq 0}$ (namely the non-negative reals is a forward invariant set for the ensuing dynamics). State σ is instrumental for the dynamic saturation limits of the augmentation scheme. In particular, given a constant vector $v \in \mathbb{R}^p$ having only positive elements, we denote by $\sqrt{\sigma v}$ the componentwise square-root of each component of v scaled by the scalar state σ. The stubborn redesigned controller is

$$\dot{z} = Fz + G \, \text{sat}_{\sqrt{\sigma v}}(y)$$

$$u = Hz + N \, \text{sat}_{\sqrt{\sigma v}}(y)$$
$$\dot{\sigma} = -\lambda \sigma + y^\top R y, \quad \sigma \in \mathbb{R}_{\geq 0}, \tag{3}$$

where the notation $\sigma \in \mathbb{R}_{\geq 0}$ emphasizes the fact that solutions are only defined with σ in the non-negative reals, so that (3) can be regarded as a constrained differential equation.

In (3), function $\text{sat}_{\sqrt{\sigma v}}$ denotes the decentralized symmetric vector-valued saturation from $\mathbb{R}^p$ to $\mathbb{R}^p$ whose components are given by $(\text{sat}_{\sqrt{\sigma v}}(y))_i = \max\{-\sqrt{\sigma v_i}, \min\{\sqrt{\sigma v_i}, y_i\}\}$ for all $i = 1, \ldots, p$. The stubborn redesign is parametrized by vector $v \in \mathbb{R}^p$, the symmetric positive semi-definite matrix R and the positive scalar $\lambda \in \mathbb{R}$. To suitably represent the redesigned closed loop, we introduce the dead-zone function $\text{dz}_{\sqrt{\sigma v}}(y) := y - \text{sat}_{\sqrt{\sigma v}}(y)$, and we define the closed-loop state $x := (x_p, z) \in \mathbb{R}^{n_p + n_c}$. Then replacing $\text{sat}_{\sqrt{\sigma v}}(y) = y - \text{dz}_{\sqrt{\sigma v}}(y)$ in (3), we may represent (1), (3) as:

$$\dot{x} = Ax - B \, \text{dz}_{\sqrt{\sigma v}}(y) + B_w w \tag{4}$$
$$y = Cx + Dw \tag{5}$$
$$\dot{\sigma} = -\lambda \sigma + y^\top R y, \quad \sigma \in \mathbb{R}_{\geq 0}, \tag{6}$$

with the following matrices:

$$\left[\begin{array}{c|c|c} A & B & B_w \\ \hline C & D & \end{array} \right]$$
$$:= \left[\begin{array}{cc|c|c} A_p + B_p N C_p & B_p H & B_p N & B_p N D_{pw} + B_{pw} \\ G C_p & F & G & G D_{pw} \\ \hline C_p & 0 & D_{pw} & \end{array} \right]. \tag{7}$$

Note that, due to Assumption 1, matrix A in (7) is Hurwitz. For the design of v, λ, and R, we rely on the Lyapunov function

$$\mathcal{V}(x, \sigma) = x^\top P x + \zeta \sigma + \mu \max\{x^\top P x - \lambda \sigma, 0\} \tag{8}$$

with $P = P^\top > 0$, and ζ and μ are positive scalars whose selection is clarified in the proof of Theorem 1. Function (8) is selected quadratic in x and linear in σ so as to obtain an LMI designed by deriving (8) along the solutions to system (4)-(6). Indeed, structure (8) allows exploiting desirable properties of both P when $x^\top P x < \lambda \sigma$ (because ζ will be selected small in the proof of Theorem 1) and $-\lambda \sigma$ when $x^\top P x > \lambda \sigma$ (because μ will be selected large in the proof of Theorem 1). The details are reported in Section III-C. Based on (8), we first impose the following condition, ensuring its decrease when σ is large (i.e., when the max function is equal to 0):

$$M_g := \text{He} \begin{bmatrix} PA - \frac{1}{2}\lambda C^\top R C + \frac{1}{2}\lambda P & -PB \\ U_g C & -U_g \end{bmatrix} < 0, \tag{9}$$

where U_g is diagonal positive definite. Conversely, for the case where σ is small (i.e., when the max function is equal to its first argument), we need to impose the next conditions

$$M_\ell := \text{He} \begin{bmatrix} PA & -PB \\ U_\ell C + Y & -U_\ell \end{bmatrix} < 0 \tag{10}$$

$$\begin{bmatrix} P & Y_{(i)}^\top \\ Y_{(i)} & \lambda^{-1} u_{\ell,i} \end{bmatrix} \geq 0, \quad \forall i = 1, \ldots, p, \tag{11}$$

where $U_\ell = \text{diag}\{u_{\ell,1}, \ldots, u_{\ell,p}\}$ is diagonal positive definite.

Within the above setting we can state and prove the following first main result, whose proof is postponed to Section III-C.

Theorem 1: Assume that there exist a scalar $\lambda > 0$, a symmetric positive definite matrix $P \in \mathbb{R}^{n \times n}$, a symmetric positive semi-definite matrix $R \in \mathbb{R}^{p \times p}$, two diagonal positive definite

matrices $U_g \in \mathbb{R}^{p \times p}$, $U_\ell \in \mathbb{R}^{p \times p}$, and a matrix $Y \in \mathbb{R}^{p \times n}$ such that inequalities (9)–(11) are satisfied. Then, selecting the entries of vector v as the inverse of the diagonal elements of U_ℓ (namely $\operatorname{diag}(v) = U_\ell^{-1}$), the closed loop (1), (3) is finite-gain exponentially input-to-state stable from w to x, namely there exist positive scalars M, $\alpha > 0$ and $\gamma > 0$ such that all solutions satisfy

$$\left|(x(t), \sqrt{\sigma(t)})\right| \le M e^{-\alpha t} \left|(x(0), \sqrt{\sigma(0)})\right| + \gamma \|w\|_2, \quad (12)$$

where $\|w\|_2$ denotes the $\mathcal{L}_\infty$ norm of w.

We provide below some information about the conservativeness of the design conditions (9)–(11).

Proposition 1: Under Assumption 1 there exist parameters P, R, U_ℓ, U_g, Y and λ satisfying the conditions of Theorem 1.

Proof: Recalling that A is Hurwitz by assumption, select P and $v > 0$ solution to $PA + A^\top P \le -vP$. Next, consider the conditions (10) and (11). With P selected above, select $Y = B^\top P - U_\ell C$. Then (10) is trivially satisfied for any $U_\ell > 0$. Then, apply the Schur complement to (11), obtaining $P - \lambda (PB - U_\ell C)_i^\top u_{\ell,i}^{-1} (PB - U_\ell C)_i \ge 0$. Fix any U_ℓ and select $\lambda < \min\{v, u_{\ell,i}/\varrho\}$, with $\varrho = \lambda_{\max}(PB - U_\ell C)^2 \lambda_{\min}(P)$. This ensures (11) is satisfied. Finally, the Schur complement of (9) gives $PA + A^\top P - \lambda C^\top R C + \lambda P + Q < 0$ with $Q = (C^\top U_g - PB) U_g^{-1} (U_g C - B^\top P)$. Using the Young inequality one obtains $Q \le 2 C^\top U_g C + 2 PB U_g^{-1} B^\top P$. Selecting $U_g > \frac{4}{v - \lambda} |PB|^2 P^{-1}$ and $R > \frac{2}{\lambda} U_g$, inequality (9) is satisfied. ∎

While Proposition 1 establishes feasibility of conditions (9)–(11), we comment here on optimality-based selections of the parameters. First observe that (9)–(11) are quasi-convex in the decision variables and correspond to a generalized eigenvalue problem in the scalar parameter λ. Indeed, except for the product λR in which λ can be absorbed in the free variable R, smaller selections of λ increase the feasibility set. Moreover, once λ has been fixed, the conditions are homogeneous in the decision variables, in the sense that if P, R, U_ℓ, U_g, Y are feasible, then cP, cR, cU_ℓ, cU_g, cY are feasible too for any $c > 0$. Therefore, an effective approach is to fix λ small enough to get feasibility of the LMIs, and then impose $P > I$ while minimizing the trace of R so that the final design is associated to a fast reduction of the stubborn parameter σ and the response quickly brings the saturation threshold to a small value that can effectively eliminate measurement outliers. This design approach is followed in the next section.

B. Simulation Example

Consider the model of the longitudinal dynamics of a fixed-wing vehicle flying at high speed, given in [25]:

$$\dot{v} = e - g \sin(\gamma) + w_1, \quad \dot{\gamma} = \ell v \sin(\theta - \gamma) - \frac{g \cos(\gamma)}{v}, \quad \dot{\theta} = q,$$

where v is the modulus of the speed, γ is the path angle, θ is the pitch angle, q is the pitch rate, g is the standard gravitational acceleration, ℓ is an aerodynamic lift coefficient, w_1 is a perturbation caused by the wind. Considering the signals e, q as control inputs and γ, θ as measured outputs, the linearization around an equilibrium $(v_0, 0, 0)$ of this model is in
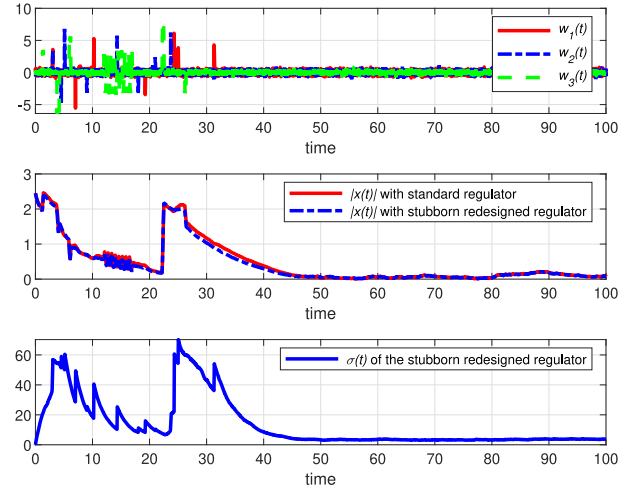

Fig. 1.   Disturbances, norm of the state, and $\sigma(t)$ (stubborn redesign).

the form (1) in which the matrices A_p, B_p, C_p are given by

$$\left[\begin{array}{c|c|c} A_p & B_p & B_{pw} \\ \hline C_p & & D_{pw} \end{array}\right] = \left[\begin{array}{ccc|cc|ccc} 0 & -g & 0 & 1 & 0 & 1 & 0 & 0 \\ g v_0^{-2} & -\ell v_0 & \ell v_0 & 0 & 0 & 0 & 0 & 0 \\ 0 & 0 & 0 & 0 & 1 & 0 & 0 & 0 \\ \hline 0 & 1 & 0 & & & 0 & 1 & 0 \\ 0 & 0 & 1 & & & 0 & 0 & 1 \end{array}\right]$$

where we supposed that measurement noise affects both outputs. Choosing $g = 1$, $v = 2$, $\ell = 0.1$, by means of pole placement we select a feedback of the form (2) with

$$\left[\begin{array}{c|c} F & G \\ \hline H & N \end{array}\right] = \left[\begin{array}{ccc|cc} -2.91 & -4.11 & -0.80 & -0.83 & 0 \\ 0.25 & -0.4 & 0 & 0.2 & 0.2 \\ -0.99 & -4.96 & -2.88 & 0 & 0 \\ \hline -2.9 & -3.9 & -0.8 & 0 & 0 \\ -1 & -4.9 & -2.8 & 0 & -0.1 \end{array}\right]$$

so that the real values of the eigenvalues of the closed-loop system are included in the set $[-3, -0.1]$. The solution of the LMI conditions (9)–(11) with a fixed $\lambda = 0.5$ provided

$$R = \begin{pmatrix} 18.4638 & 2.5576 \\ 2.5576 & 5.9588 \end{pmatrix}, \quad v = \begin{pmatrix} 0.1978 \\ 0.1300 \end{pmatrix}.$$

Fig. 1 shows the simulations, where the adaptive saturation level σ, initialized at zero, is clearly excited by the outliers affecting the measurements before $t = 35\,\mathrm{s}$ and then becomes quite small when no other outliers occur after $t = 35\,\mathrm{s}$. The outliers' effect is clearly attenuated, as illustrated by the middle plot. Based on Fig. 1, we computed the integrals of $|x(t)|$ in the interval $t \in [0, 60]\,\mathrm{s}$ for the standard regulator case and the stubborn redesigned regulator case, which are equal to 42.4572 and 39.4415, respectively.

C. Proof of Theorem 1

Consider the candidate Lyapunov function $\mathcal{V}$ in (8). Such a function is linear in σ and quadratic in x. Furthermore, recalling that $\sigma \in \mathbb{R}_{\ge 0}$, we deduce that $\mathcal{V}$ is positive definite on $\mathbb{R}^n \times \mathbb{R}_{\ge 0}$ and satisfies the bounds

$$\alpha_1 |(x, \sqrt{\sigma})|^2 \le \mathcal{V}(x, \sigma) \le \alpha_2 |(x, \sqrt{\sigma})|^2, \quad (13)$$

where $\alpha_1 := \min\{\lambda_{\min}(P), \zeta\}$, and $\alpha_2 := \max\{(1 + \mu)\lambda_{\max}(P), \zeta\}$ stem from upper and lower bounding the various terms in (8). Similar to [13, Proof of Th. 1], one can observe that function $\mathcal{V}(x, \sigma)$ is not differentiable in the set of measure zero where $x^\top Px - \lambda\sigma = 0$. However, it is continuous and locally Lipschitz. Therefore, proceeding as in [13], due to continuity of the closed-loop dynamics (1), (3), it is enough to ensure suitable decrease conditions of $\mathcal{V}$ for almost all points of the state space (see also the recent results of [26] for an alternative proof of this fact). To check our Lyapunov conditions almost everywhere, we split the analysis in two cases: (C1) $x^\top Px < \lambda\sigma$ and (C2) $x^\top Px > \lambda\sigma$.

(C1). In this case, (8) yields $\mathcal{V}(x, \sigma) = x^\top Px + \zeta\sigma$, whose directional derivative along dynamics (4)–(6) reads

$$
\dot{\mathcal{V}}(x, \sigma) = 2\left(x^\top PAx - x^\top PB \, \mathrm{dz}_{\sqrt{\sigma v}}(y) + x^\top PB_w w\right) \\
- 2\lambda\zeta\sigma + 2\zeta y^\top Ry. \tag{14}
$$

We use [27, Lemma 1.6] with respect to $\mathrm{dz}_{\sqrt{\sigma v}}$, leading to the following regional sector condition (we use dz here and below as a shortcut notation for $\mathrm{dz}_{\sqrt{\sigma v}}(y)$): $\mathrm{dz}^\top U_\ell(y + Qx - \mathrm{dz}) \geq 0$, which holds for any positive definite diagonal matrix $U_\ell \in \mathbb{R}^{p \times p}$, any matrix $Q \in \mathbb{R}^{p \times n}$ and any x satisfying $-\sqrt{\sigma v_i} \leq Q_{(i)}x \leq \sqrt{\sigma v_i}$.

Let us now consider (11) and notice that, with the selection $Y = U_\ell Q$, and recalling the selection $\mathrm{diag}(v)^{-1} = U_\ell$ from the theorem statement, a Schur complement provides, $P - \lambda v_i^{-1} Q_{(i)}^\top Q_{(i)} \geq P - \lambda u_{\ell,i} Q_{(i)}^\top Q_{(i)} \geq 0$. This inequality, combined with the inequality pertaining case (C1), provides

$$
\lambda v_i^{-1}|Q_{(i)}x|^2 = \lambda v_i^{-1} x^\top Q_{(i)}^\top Q_{(i)} x \leq x^\top Px \leq \lambda\sigma, \tag{15}
$$

which ensures that the regional sector condition holds, because $-\sqrt{\sigma v_i} \leq Q_{(i)}x \leq \sqrt{\sigma v_i}$. Based on the above reasoning, we may construct the following bound on $\dot{\mathcal{V}}$, stemming from (14)

$$
\dot{\mathcal{V}} \leq \dot{\mathcal{V}} + 2\,\mathrm{dz}^\top U_\ell(y + Qx - \mathrm{dz}) \\
= 2\left(x^\top PAx - x^\top PB\,\mathrm{dz} + x^\top PB_w w\right) - \lambda\zeta\sigma \tag{16} \\
+ \zeta y^\top Ry + 2\,\mathrm{dz}^\top U_\ell(y + Qx - \mathrm{dz}).
$$

To suitably bound the right-hand side of (16), we may use Young's inequality multiple times to construct a large enough scalar κ_ℓ such that, for any $\varepsilon > 0$, the following bounds hold:

$$
x^\top PB_w w \leq \varepsilon|x|^2 + \frac{\kappa_\ell}{\varepsilon}|w|^2, \tag{17}
$$

$$
y^\top Ry \leq (1 + \varepsilon)x^\top C^\top RCx + \kappa_\ell \frac{1+\varepsilon}{\varepsilon}|w|^2 \tag{18}
$$

$$
\mathrm{dz}_{\sqrt{\sigma v}}(Cx + Dw)^\top U_\ell Dw \leq \varepsilon|x|^2 + \kappa_\ell \frac{1+\varepsilon}{\varepsilon}|w|^2. \tag{19}
$$

Finally, denoting $\xi := (x, \mathrm{dz}_{\sqrt{\sigma v}}(y))$ and combining bounds (16)–(19), we obtain, after recalling that we fixed $Y = U_\ell Q$, and choosing $\zeta = \varepsilon$,

$$
\dot{\mathcal{V}}(x, \sigma) \leq \xi^\top \left(M_\ell + \varepsilon \begin{bmatrix} 4I + (1+\varepsilon)C^\top RC & 0 \\ 0 & 0 \end{bmatrix}\right)\xi \\
- 2\varepsilon\lambda\sigma + \bar{\kappa}_\ell|w|^2, \tag{20}
$$

where $\bar{\kappa}_\ell := \frac{3\kappa_\ell}{\varepsilon}(1 + \varepsilon)$.

(C2). In this case, due to $x^\top Px > \lambda\sigma$, and recalling the selection $\zeta = \varepsilon$ performed above, definition (8) yields $\mathcal{V}(x, \sigma) = x^\top Px + \varepsilon\sigma + \mu(x^\top Px - \lambda\sigma) = (1 + \mu)x^\top Px +$

$(\varepsilon - \lambda\mu)\sigma$, whose directional derivative along dynamics (4)–(6) reads

$$
\dot{\mathcal{V}}(x, \sigma) = 2(1 + \mu)x^\top P\dot{x} + (\varepsilon - \lambda\mu)\dot{\sigma} \\
= 2(1 + \mu)\left(x^\top PAx - x^\top PB\,\mathrm{dz}_{\sqrt{\sigma}}(y) + x^\top PB_w w\right) \\
+ (\lambda\mu - \varepsilon)\lambda\sigma - (\lambda\mu - \varepsilon)y^\top Ry. \tag{21}
$$

We use [27, Lemma 1.4] with respect to $\mathrm{dz}_{\sqrt{\sigma v}}$, leading to the global sector condition: $\mathrm{dz}^\top U_g(Cx + Dw - \mathrm{dz}) \geq 0$ for any positive diagonal matrix $U_g \in \mathbb{R}^{p \times p}$, where we use once again the placeholder dz instead of $\mathrm{dz}_{\sqrt{\sigma v}}(y)$, to simplify the notation. Moreover, using the assumed inequality for case (C2) we obtain

$$
0 \leq \lambda\mu(x^\top Px - \lambda\sigma) \leq \lambda\mu x^\top Px - \mu\lambda^2\sigma. \tag{22}
$$

Summing up the above sector condition with inequality (22) and with (21), we obtain the following bound

$$
\dot{\mathcal{V}} \leq \dot{\mathcal{V}} + 2\mu\,\mathrm{dz}^\top U_g(Cx + Dw - \mathrm{dz}) + 2\lambda\mu(x^\top Px - \lambda\sigma) \\
= 2(1 + \mu)\left(x^\top PAx - x^\top PB\,\mathrm{dz} + x^\top PB_w w\right) \\
+ \lambda\mu x^\top Px - \varepsilon\lambda\sigma - (\lambda\mu - \varepsilon)y^\top Ry \\
+ 2\mu\,\mathrm{dz}^\top U_g(Cx + Dw - \mathrm{dz}). \tag{23}
$$

To suitably bound the right-hand side of (23), we first assume for simplicity $\mu > \varepsilon$ (eventually, μ will be selected sufficiently large) and then proceeding as in (17)–(19), we use repeatedly Young's inequality to show that there exists κ_g such that, for each $\varepsilon > 0$, the following bounds hold:

$$
x^\top PB_w w \leq \varepsilon|x|^2 + \frac{\kappa_g}{\varepsilon}|w|^2, \tag{24}
$$

$$
-y^\top Ry \leq -(1 - \varepsilon)x^\top C^\top RCx + \kappa_g \frac{1+\varepsilon}{\varepsilon}|w|^2, \tag{25}
$$

$$
\mathrm{dz}_{\sqrt{\sigma v}}(Cx + Dw)^\top U_g Dw \leq \varepsilon|x|^2 + \kappa_g \frac{1+\varepsilon}{\varepsilon}|w|^2. \tag{26}
$$

Finally, denoting again $\xi := (x, \mathrm{dz}_{\sqrt{\sigma v}}(y))$ and combining bounds (23)–(26), we obtain the following estimate

$$
\dot{\mathcal{V}}(x, \sigma) \leq \xi^\top \left(\mu M_g + \begin{bmatrix} (1+2\mu)\varepsilon I & 0 \\ 0 & 0 \end{bmatrix} + \mathrm{He}\begin{bmatrix} PA + \frac{\varepsilon}{2}C^\top RC & 0 \\ -B^\top P & 0 \end{bmatrix}\right)\xi \\
- \varepsilon\lambda\sigma + \bar{\kappa}_g|w|^2, \tag{27}
$$

where $\bar{\kappa}_g = (3\mu - 2 + 5\frac{\mu}{\varepsilon})\kappa_g > 0$ and M_g, as defined in (9), is negative definite.

Summary: The two bounds (20) and (27) obtained for cases (C1) and (C2), respectively, allow selecting a large enough μ and a small enough ε such that the matrices in the quadratic forms appearing in (20) and (27) are both negative definite. Representing $\sigma = \sqrt{\sigma}^2$, we obtain that there exists a small enough $\bar{\varepsilon} > 0$ and a large enough $\bar{\kappa}$ such that, for all of the considered cases (namely for almost all (x, σ)), we have

$$
\dot{\mathcal{V}}(x, \sigma) \leq -\bar{\varepsilon}\left|(x, \sqrt{\sigma})\right|^2 + \bar{\kappa}|w|^2, \tag{28}
$$

which, together with (13) shows that $\mathcal{V}$ is an ISS Lyapunov function proving bound (12), and thus completing the proof.[1]

---

[1]The reader is referred to [12] for basic concepts about ISS Lyapunov functions and to [26] for nonsmooth ISS Lyapunov functions.

IV. LMI-BASED DEAD-ZONE REDESIGN

A. Design Paradigm and Main Result

We augment here controller (2) with an adaptive dead-zone having a dynamic dead-zone threshold σ, as follows

$$\dot{z} = Fz + G\,\mathrm{dz}_{\sqrt{\sigma v}}(y)$$
$$u = Hz + N\,\mathrm{dz}_{\sqrt{\sigma v}}(y)$$
$$\dot{\sigma} = -\lambda\sigma + y^\top Ry, \ \sigma \in \mathbb{R}_{\geq 0}, \tag{29}$$

where $v \in \mathbb{R}^p$ is a constant vector having positive elements and $\sqrt{\sigma v} \in \mathbb{R}_{\geq 0}$ is the component-wise square root of vector σv. The dynamics of σ ensures by construction the forward invariance of the non-negative real axis $\mathbb{R}_{\geq 0}$ for state σ. Therefore $\sqrt{\sigma v}$ is well defined. The dead-zone augmentation (29) depends on the following design parameters: the positive scalar λ and the symmetric positive semi-definite matrix $R \in \mathbb{R}^{p \times p}$.

Paralleling the derivations in (4)-(7), defining the combined state $x = (x_p, z) \in \mathbb{R}^{n_p + n_c}$, the closed-loop system (1), (29) can be written in the following compact form:

$$\dot{x} = Ax - B\,\mathrm{sat}_{\sqrt{\sigma v}}(Cx + Dw) + B_w w \tag{30}$$
$$y = Cx + Dw \tag{31}$$
$$\dot{\sigma} = -\lambda\sigma + y^\top Ry, \quad \sigma \in \mathbb{R}_{\geq 0}, \tag{32}$$

with the same matrices as those defined in (7). In particular, we recall that A is Hurwitz due to Assumption 1.

For analyzing the closed-loop properties of (30), (32) we rely on the following Lyapunov function (with a slight abuse of notation, to keep our notation simple, we use the same symbols $\mathcal{V}$, M_g and U_g as in Section III)

$$\mathcal{V}(x, \sigma) = x^\top Px + 2\sigma, \tag{33}$$

where $P = P^\top > 0$ is to be designed. For ensuring suitable decrease properties of $\mathcal{V}$ it is here enough to impose only one condition, corresponding to

$$M_g := \mathrm{He}\begin{bmatrix} PA + \frac{1}{2}C^\top RC & -PB \\ U_g C & -U_g(1+\lambda) \end{bmatrix} < 0, \tag{34}$$

where U_g is a diagonal positive definite matrix.

We can then state the following main result, whose proof is postponed to Section IV-C.

Theorem 2: If there exist a symmetric positive definite matrix $P \in \mathbb{R}^{n \times n}$, a symmetric positive semi-definite matrix $R \in \mathbb{R}^{p \times p}$, a diagonal positive definite matrix $U_g \in \mathbb{R}^{p \times p}$ and a scalar $\lambda > 0$ satisfying (34), then selecting v as the diagonal elements of U_g^{-1} (namely $\mathrm{diag}(v) = U_g^{-1}$) the closed loop (1), (29) is finite-gain exponentially input-to-state stable from w to x, namely there exist positive scalars $M, \alpha > 0$ and $\gamma > 0$ such that all solutions satisfy bound (12).

The design condition (34) of Theorem 2 is quasi-convex in the variable λ. We prove below that, under Assumption 1, these conditions are always feasible.

Proposition 2: Under Assumption 1 there exist parameters P, R, λ and U_g satisfying the conditions of Theorem 2.

Proof: It has been observed that Assumption 1 implies that A be Hurwitz. Then there exists a small enough R and a positive definite P such that $A^\top P + PA + C^\top RC < 0$. Taking $U_g = I$ and λ large enough, constraint (34) is clearly satisfied. ∎

The main rationale of using the proposed dead-zone redesign (29) is to attenuate the effect of the noise w from y to
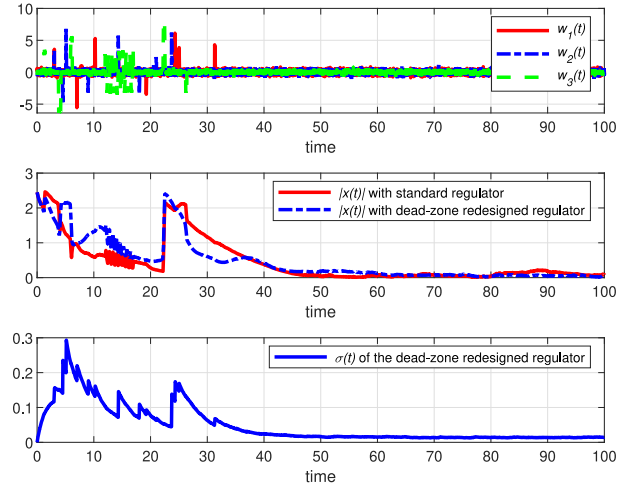

Fig. 2. Disturbances, norm of the state, and $\sigma(t)$ (dead-zone redesign).

the control u (in particular when y is close to zero and hence mainly composed by noise w). In terms of design guidelines, since (34) is homogeneous for a fixed λ, a possible strategy for maximizing the effectiveness of the dead-zone redesign is to fix λ, then impose $P < I$ (which does not affect feasibility due to the homogeneity property) and then maximize the trace of a diagonal R, possibly promoting the directions corresponding to the sensors most affected by persistent noise.

B. Simulation Example

We consider the same example of Section III-B. For a dead-zone redesign, we obtain

$$R = \begin{pmatrix} 0.0294 & 0.0017 \\ 0.0017 & 0.0617 \end{pmatrix}, \ v = \begin{pmatrix} 1.6086 \\ 2.6432 \end{pmatrix},$$

after solving the LMI condition (34) with $\lambda = 0.5$. Simulation results are shown in Fig. 2 with the same initial conditions and noises of Fig. 1. The bottom plot clearly shows that dead-zone level σ is highly excited by the outliers occurring in the first interval, where the redesign effect is not advantageous, especially with the repeated outliers between $t = 10\,\mathrm{s}$ and $t = 20\,\mathrm{s}$, because it is not suited for these disturbances. Instead, the redesign is very effective at the steady state, where it provides desirable reduction of the steady-state error caused by persistent noise (see, especially, the middle response in the interval $t \in [80, 100]\,\mathrm{s}$). We computed the integrals of $|x(t)|$ in the interval $t \in [60, 100]\,\mathrm{s}$ for the standard regulator and the dead-zone redesigned regulator, which are given by 3.6459 and 2.5558, respectively. This confirms the fact that the stubborn redesign is suitable for improving the response to outliers (compare with Fig. 1), and the dead-zone redesign is suitable for improving the response to persistent noise.

C. Proof of Theorem 2

Differently from the proof of Theorem 1, there is no need for this proof to split the analysis in two cases, and only one set of inequalities is sufficient to establish the result. Consider the candidate Lyapunov function $\mathcal{V}$ in (33) and note that the fact that $\sigma \in \mathbb{R}_{\geq 0}$ implies that $\mathcal{V}$ is positive definite on $\mathbb{R}^n \times \mathbb{R}_{\geq 0}$ satisfies bound (13), with $\alpha_1 := \min\{\lambda_{\min}(P), 2\}$, and $\alpha_2 := \max\{\lambda_{\max}(P), 2\}$ (namely $\mathcal{V}$ it is positive definite

and radially unbounded). The time-derivative of $\mathcal{V}$ along the solutions of (30), (32) reads:

$$\dot{\mathcal{V}}(x, \sigma) = 2x^\top P\dot{x} + 2\dot{\sigma} = 2x^\top PAx - 2x^\top PB \, \mathrm{sat}_{\sqrt{\sigma v}}(y)$$
$$+ 2x^\top PB_w w - 2\lambda\sigma + 2y^\top Ry. \quad (35)$$

By exploiting the sector properties and global boundedness of $\mathrm{sat}_{\sqrt{\sigma v}}(y)$ we obtain the following two conditions:

- $\mathrm{sat}_{\sqrt{\sigma v}}(y)^\top U_g(y - \mathrm{sat}_{\sqrt{\sigma v}}(y)) \geq 0$, for any positive diagonal matrix $U_g \in \mathbb{R}^{p \times p}$ from [27, Lemma 1.4];
- $\lambda(\sigma - \mathrm{sat}_{\sqrt{\sigma v}}(y)^\top U_g \, \mathrm{sat}_{\sqrt{\sigma v}}(y)) \geq 0$.

Summing up the above conditions to expression (35), we obtain the following bound (where we use "sat" in place of "$\mathrm{sat}_{\sqrt{\sigma v}}(y)$" to make the notation compact):

$$\dot{\mathcal{V}} \leq \dot{\mathcal{V}} + 2\,\mathrm{sat}^\top U_g(y - \mathrm{sat}) + 2(1-\varepsilon)\lambda(\sigma - \mathrm{sat}^\top U_g\,\mathrm{sat})$$
$$= 2x^\top PAx - 2x^\top PB\,\mathrm{sat} + 2x^\top PB_w w$$
$$+ 2y^\top Ry + 2\,\mathrm{sat}^\top U_g(Cx + Dw - \mathrm{sat})$$
$$- 2\varepsilon\lambda\sigma - 2(1-\varepsilon)\lambda\,\mathrm{sat}^\top U_g\,\mathrm{sat}, \quad (36)$$

where $\varepsilon > 0$ is selected below. To suitably bound the right-hand side of (36), we use repeatedly Young's inequality to show that there exists κ_g such that, for each $\varepsilon > 0$, the following bounds hold:

$$x^\top PB_w w \leq \varepsilon|x|^2 + \frac{\kappa_g}{\varepsilon}|w|^2, \quad (37)$$
$$y^\top Ry \leq (1+\varepsilon)x^\top C^\top RCx + \kappa_g\frac{1+\varepsilon}{\varepsilon}|w|^2, \quad (38)$$
$$\mathrm{sat}_{\sqrt{\sigma v}}(Cx + Dw)^\top U_g Dw \leq \varepsilon|x|^2 + \kappa_g\frac{1+\varepsilon}{\varepsilon}|w|^2. \quad (39)$$

Finally, denoting $\xi := (x, \mathrm{sat}_{\sqrt{\sigma v}}(y))$ and combining bounds (36)–(39), we obtain the following estimate

$$\dot{\mathcal{V}}(x, \sigma) \leq \xi^\top\left(M_g + \varepsilon\begin{bmatrix} 2I + C^\top RC & 0 \\ 0 & 2\lambda U_g \end{bmatrix}\right)\xi - 2\varepsilon\lambda\sigma + \bar{\kappa}_g|w|^2$$

where $\bar{\kappa}_g = (2 + \frac{3}{\varepsilon})\kappa_g > 0$ and M_g, as defined in (34), is negative definite. The last inequality allows selecting a small enough ε such that the matrix in the quadratic form is negative definite (because of the strict inequality in (34)). Representing $\sigma = \sqrt{\sigma}^2$, it is then immediate to obtain, for a small enough $\bar{\varepsilon} > 0$ and a large enough $\bar{\kappa}$ the bound in (28) for all (x, σ). This bound, together with (13) (which was proven at the beginning of the proof) shows that $\mathcal{V}$ is an ISS Lyapunov function proving bound (12), and thus completing the proof.

V. Conclusion

We rigorously and successfully addressed performance improvement for linear dynamic output feedbacks with stubborn and dead-zone redesigns. Future work includes comparing the nominal and redesigned feedbacks by generalizing the results in [15, Sec. III-B, p. 671 and Sec. IV-B, p. 674] and the output feedback for nonlinear systems, possibly with multi-variable threshold dynamics.

References

[1] P. Gahinet and P. Apkarian, "A linear matrix inequality approach to $H\infty$ control," *Int. J. Robust Nonlinear Control*, vol. 4, no. 4, pp. 421–448, 1994.

[2] J. C. Doyle, B. A. Francis, and A. R. Tannenbaum, *Feedback Control Theory*. Chelmsford, MA, USA: Courier Corp., 2013.

[3] S. Skogestad and I. Postlethwaite, *Multivariable Feedback Control: Analysis and Design*, vol. 2. Chichester, U.K.: Wiley, 2007.

[4] G. Marro, F. Morbidi, L. Ntogramatzidis, and D. Prattichizzo, "Geometric control theory for linear systems: A tutorial," in *Proc. 19th Int. Symp. Math. Theory Netw. Syst.*, vol. 5, 2010, pp. 1579–1590.

[5] B. A. Francis and W. M. Wonham, "The internal model principle for linear multivariable regulators," *Appl. Math. Optim.*, vol. 2, no. 2, pp. 170–194, 1975.

[6] C. Scherer, P. Gahinet, and M. Chilali, "Multiobjective output-feedback control via LMI optimization," *IEEE Trans. Autom. Control*, vol. 42, no. 7, pp. 896–911, Jul. 1997.

[7] C. Prieur and A. R. Teel, "Uniting local and global output feedback controllers," *IEEE Trans. Autom. Control*, vol. 56, no. 7, pp. 1636–1649, Jul. 2011.

[8] F. Fichera, C. Prieur, S. Tarbouriech, and L. Zaccarian, "Improving the performance of linear systems by adding a hybrid loop: The output feedback case," in *Proc. Amer. Control Conf.*, 2012, pp. 3192–3197.

[9] G. Zhao, D. Nesic, Y. Tan, and J. Wang, "Improving $\mathcal{L}2$ gain performance of linear systems by reset control," *IFAC Proc. Vol.*, vol. 47, no. 3, pp. 6400–6405, 2014.

[10] A. Alessandri and R. G. Sanfelice, "Hysteresis-based switching observers for linear systems using quadratic boundedness," *Automatica*, vol. 136, Feb. 2022, Art. no. 109982.

[11] D. Astolfi, R. Postoyan, and D. Nešić, "Uniting observers," *IEEE Trans. Autom. Control*, vol. 65, no. 7, pp. 2867–2882, Jul. 2020.

[12] E. D. Sontag, "Input to state stability: Basic concepts and results," in *Nonlinear and Optimal Control Theory*. Berlin, Germany: Springer, 2008, pp. 163–220.

[13] A. Alessandri and L. Zaccarian, "Stubborn state observers for linear time-invariant systems," *Automatica*, vol. 88, pp. 1–9, Feb. 2018.

[14] D. Astolfi, A. Alessandri, and L. Zaccarian, "Stubborn ISS redesign for nonlinear high-gain observers," *IFAC-PapersOnLine*, vol. 50, no. 1, pp. 15422–15427, 2017.

[15] D. Astolfi, A. Alessandri, and L. Zaccarian, "Stubborn and dead-zone redesign for nonlinear observers and filters," *IEEE Trans. Autom. Control*, vol. 66, no. 2, pp. 667–682, Feb. 2021.

[16] M. Cocetti, S. Tarbouriech, and L. Zaccarian, "High-gain dead-zone observers for linear and nonlinear plants," *IEEE Contr. Syst. Lett.*, vol. 3, pp. 356–361, 2019.

[17] G. Casadei, D. Astolfi, A. Alessandri, and L. Zaccarian, "Synchronization of interconnected linear systems via dynamic saturation redesign," *IFAC-PapersOnLine*, vol. 52, no. 16, pp. 622–627, 2019.

[18] G. Casadei, D. Astolfi, A. Alessandri, and L. Zaccarian, "Synchronization in networks of identical nonlinear systems via dynamic dead zones," *IEEE Contr. Syst. Lett.*, vol. 3, pp. 667–672, 2019.

[19] J. Mao, D. Ding, and G. Wei, "Distributed stubborn-set-membership filtering with a dynamic event-based scheme: The Takagi-Sugeno fuzzy framework," *Int. J. Adapt. Control Signal Process.*, vol. 35, no. 4, pp. 513–531, 2021.

[20] M. Zareian and M. Shafiei, "A modification in the structure of low-power high-gain observers to improve the performance in the presence of disturbances and measurement noise," *Eur. J. Control*, vol. 58, pp. 278–288, 2021.

[21] H. Fang, M. A. Haile, and Y. Wang, "Robust extended Kalman filtering for systems with measurement outliers," *IEEE Trans. Control Syst. Technol.*, vol. 30, no. 2, pp. 795–802, Mar. 2022.

[22] J. Sun, B. Shen, J. Qi, and Y. Liu, "Stubborn H∞ state estimation for nonlinear distributed parameter systems subject to measurement outliers," *Int. J. Robust Nonlinear Control*, vol. 32, no. 1, pp. 13–28, 2022.

[23] L. Ma, Z. Wang, H. Liu, F. E. Alsaadi, and F. E. Alsaadi, "Neural-network-based filtering for a general class of nonlinear systems under dynamically bounded innovations over sensor networks," *IEEE Trans. Netw. Sci. Eng.*, vol. 9, no. 3, pp. 1395–1408, May/Jun. 2022.

[24] S. Boyd, L. El Ghaoui, E. Feron, and V. Balakrishnan, *Linear Matrix Inequalities in System and Control Theory* (Studies in Applied Mathematics), vol. 15. Philadelphia, PA, USA: SIAM, 1994.

[25] D. Astolfi and L. Praly, "Integral action in output feedback for multi-input multi-output nonlinear systems," *IEEE Trans. Autom. Control*, vol. 62, no. 4, pp. 1559–1574, Apr. 2017.

[26] M. D. Rossa, R. Goebel, A. Tanwani, and L. Zaccarian, "Piecewise structure of Lyapunov functions and densely checked decrease conditions for hybrid systems," *Math. Control Signals Syst.*, vol. 33, pp. 123–149, Feb. 2021.

[27] S. Tarbouriech, G. Garcia, J. M. G. Da Silva, Jr., and I. Queinnec, *Stability and Stabilization of Linear Systems With Saturating Actuators*. London, U.K.: Springer, 2011.